



PZT–PDMS composite for active damping of vibrations

Satinder K. Sharma^{a,b}, Himani Gaur^a, Manish Kulkarni^a, Ganesh Patil^a, Bishakh Bhattacharya^c,
Ashutosh Sharma^{a,*}

^a Thematic Unit of Excellence, Nanoscience and Nanotechnology on Soft Nanofabrication and Department of Chemical Engineering, Indian Institute of Technology (IIT), Kanpur 208 016, Uttar Pradesh, India

^b School of Computing and Electrical Engineering, Indian Institute of Technology (IIT), Mandi 175 001, Himachal Pradesh, India

^c Department of Mechanical Engineering, Indian Institute of Technology (IIT), Kanpur 208 016, Uttar Pradesh, India

ARTICLE INFO

Article history:

Received 15 March 2012

Received in revised form 19 December 2012

Accepted 3 January 2013

Available online 16 January 2013

Keywords:

A. Smart materials

B. Mechanical properties

C. Complex moduli

D. Non-destructive testing

E. Casting

ABSTRACT

A Lead Zirconate-Titanate (PZT)/poly-dimethylsiloxane (PDMS) based flexible composite is synthesized and investigated for its potential in significantly enhancing the vibration damping capability along with its tunable properties. Rheologically and functionally different PZT/PDMS composites are prepared by dispersing different volume fractions of piezoelectric soft/hard PZT and Fe particles in a cross-linked PDMS matrix. It is observed that passive damping increases with increase in the soft PZT volume fraction from 0 to 0.32. This effect becomes more prominent after poling the composite at optimum conditions. The loss factor depends on the viscoelastic properties of the PDMS, homo and hetero-particle connectivity in the composite, and polarization and localization of the PZT particles in composite. Rheological analysis of the composite shows that the material loss factor ($\tan \delta$) increases linearly from ~ 0.3 to 0.75 along with a broadening of the peak when the PZT volume fraction is increased from 0 to 0.32. Maximum structural damping (η) is obtained at 0.32 (V/V) of the soft-PZT as measured by the Oberst beam technique. This effect becomes more pronounced after a poling treatment. The X-ray diffraction results indicate that the dispersed PZT particles in PDMS matrix have the lattice parameters of $a = 5.84 \text{ \AA}$, $c = 14.41 \text{ \AA}$ and (001) orientation. Further, after poling treatment, the dielectric constant and the piezoelectric coefficient (d_{33}) for soft (submicron) PZT filler particles in PDMS matrix tend to be higher than those for hard PZT. The soft PZT/PDMS composite shows better performance as a damper than the hard, PZT composite.

© 2013 Elsevier Ltd. All rights reserved.

1. Introduction

The technological and environmental trends of the past few decades indicate that the damping of mechanical vibrations is becoming increasingly important for energy efficient systems. Vibrations not only result in the fatigue and failure of engineering systems, but also generate noise pollution. Furthermore, vibrations control in dynamic components of a mechanical system is of great importance to reduce heat losses and wear and tear of the components. Thus, much effort has been expended in developing new damping materials to produce efficient structural damping [1–5]. Lead Zirconate Titanate (PZT) is a compound of Lead Zirconate and Lead Titanate with molecular formula $\text{Pb}[\text{Zr}_{1-x}\text{Ti}_x]\text{O}_3$. It is known for its excellent piezoelectric properties, high Curie temperature, spontaneous polarization and high electromechanical coupling coefficient. Thus, it is widely used commercially for acoustic and vibration damping applications [6]. However, low

flexibility, high fragility and brittleness of PZT make it difficult to be applied as a damping layer over complex curved surfaces and limit its use in broad-band vibration control. Hence, piezoelectric–polymer composite materials are being studied as an alternative material for damping. The composite is readily tailorable, exhibits damping behavior of viscoelastic materials, high loss factor, broad distribution of relaxation time [6,7] and specialized damping mechanism based on energy conversion [8]. In these systems, the mechanical vibration energy of viscoelastic polymer matrix is first transmitted to the embedded piezoelectric ceramic powder particles and then gets converted into electrical energy by the piezoelectric effect. This electrical energy is transmitted further through the network of electro-conductive particles inside the viscoelastic matrix [8,9]. Furthermore, adding an electrical network with piezoelectric–polymer composite (shunting) modifies its electrical and mechanical impedance and thus, leads to additional mechanical damping analogous to viscoelastic materials [10]. PZT–Polymer composites have attracted much attention as they have higher strength-to-weight and stiffness-to-weight ratio [11]. Efforts have been made to develop PZT–polymer composites by two methods: (a) dispersion of PZT particles in polymer matrix,

* Corresponding author. Tel.: +91 512 2597026; fax: +91 512 2590104.

E-mail addresses: satinder@iitmandi.ac.in (S.K. Sharma), ashutos@iitk.ac.in (A. Sharma).

and (b) lamellar PZT–polymer structures [7]. Each of these methods has its own advantages and disadvantages. The dispersion of PZT in polymer matrix offers a synergy of PZT and polymeric properties as the polymer phase reduces the density of the composite but increases its flexibility, which is favorable for mechanical damping. The amalgamation of a small fraction of piezoelectric ceramics and polymers result in soft composites with limited piezoelectric properties. Moreover, the inter-connectivity of piezoelectric particles is poor and hence, such composites show weak piezoelectric effect. However, heat generation at the PZT polymer interface because of friction between these two phases increases the passive damping at the cost of mechanical energy. Presently, the relationship between electric polarization and orientation of ceramic particles in the polymer matrix is an intriguing issue [12]. Also, only a few polymers like Polyvinylidene fluoride (PVDF) possess the required dielectric constant and dielectric strength to permeate the electric field necessary for the poling of PZT particles without dielectric breakdown and facilitate active vibration damping in these composites [13]. Using a lamellar PZT–polymer structures ensures connectivity of the piezoelectric phase in 2-d plane, however these composites exhibit limited flexibility due to the stiffness of the PZT layers and thus, in general, cannot be used for damping of vibration for curved body surfaces. In addition, very small PZT–polymer interface of the laminate (as compared to dispersion of PZT particles in polymer matrix) reduces the passive damping properties of this composite [11]. There are a few studies on the lamellar Polydimethylsiloxane (PDMS)–PZT composites for damping applications [14]. In the last few years, a great deal of effort has been devoted to the development of ceramic–polymer composites by various researchers. Newham et al. [15] succeeded in preparing a composite of PZT silicone rubber and PZT–epoxy by the coral replamine process. Shrout et al. [16] investigated a composite of the same material prepared by the burned-out plastic sphere (BURPS) technique. Safari et al. [17] prepared a composite by arranging PZT spheres in a close-packed monolayer in a flat plastic container and pouring polymer over the spheres. More recently, Furukawa et al. [18] studied the piezoelectric properties for the composite system of PZT ceramics and polymers such as polyvinylidene fluoride (PVDF), polyethylene (PE) and polyvinyl alcohol (PVA). Ahmad et al. [3] presented the quantitative analysis of relative permittivity, dielectric loss factor, piezoelectric charge coefficient and Young's modulus of PZT/PVDF diphasic ceramic–polymer composite as a function of volume fraction of PZT in different compositions. However, to our knowledge in none of these studies the viscoelastic properties of the polymer were varied systematically and its effect on the damping properties of the composite is reported. Taking these issues into consideration, the composites were prepared by the dispersion of soft/hard-PZT and Fe particles in PDMS matrix. The mechanical damping, rheological, crystalline and piezoelectric properties before and after poling were studied. PDMS is known for its good thermal and oxidation stability, water resistance, chain flexibility and sound absorption capacity. Most importantly, one can easily control its viscoelastic properties by changing the crosslinking percentage and still retain its flexibility and binding properties [19]. The viscous properties of PDMS are especially useful for passive damping of mechanical vibrations. Use of viscoelastic materials in passive damping mechanism has proven to be a reliable method towards improved structural dynamics. Therefore, the viscoelasticity of PDMS and piezoelectricity of PZT in a composite system may be considered as a prospective candidate for flexible damping layer. Until now, no report has been available on the rheological analysis of a composite containing piezoelectric material. Rheology may prove to be a very useful tool as it provides direct insight into the damping properties of the composite such as material loss factor, loss and storage shear moduli. The higher the viscous modulus and material

loss factor of a material, the better is the damping capacity of the material [20]. One can easily detect the frequency response of the material loss factor, which otherwise is a difficult task for composites. Similarly, the domains of soft and hard PZT fillers dispersed in the PDMS matrix, switching with the domain wall motion, markedly affects the dielectric and piezoelectric properties [21]. The piezoelectric constant (d_{33}) is computed by d_{33} -meter based on the direct effect. The d_{33} meter applies a periodic weak stress to the sample and detects an induced polarization. However, the origin of variation in dielectric constant and piezoelectric property for PZT–PDMS composite system has not been well established till date [22]. Moreover, the ceramic/polymer composites with varying ceramic content under optimum conditions have not been investigated extensively.

With this perspective, in the present work, soft PZT, hard PZT and ferrous particles are dispersed in the PDMS matrix and the rheological properties, damping behavior and structural loss factor are studied by using the Rheometer and the conventional Oberst beam technique respectively. Subsequently, the effect of poling on piezoelectric ceramic–polymer composite is investigated. The effect on the crystalline character of composite and the shape and size of particles before and after poling treatment are investigated by X-ray and FESEM analysis. The dielectric constant and the piezoelectric coefficient of the composite are computed by impedance analyzer and d -m respectively with soft PZT filler particles.

2. Materials and methods

2.1. Sample preparation

Soft PZT powder (donor doped lanthanides of grain size $<1\ \mu\text{m}$ and higher coupling factor), purchased from M/S Concord Electroceraic Ltd., New Delhi, India was mixed with Sylgard-184 (a two-part PDMS elastomer, Dow Chemicals, USA) to prepare PDMS–PZT thick films. Addition of 5% crosslinking agent to the mixture followed by thermal curing at $120\ ^\circ\text{C}$ for 24 h resulted in the crosslinking of PDMS chains. The paste was vigorously hand mixed in a beaker for nearly 15 min followed by ultrasonication in a water bath for 5 min. The bubbles formed during mixing were removed by desiccating the mixture for 15 min under vacuum. Then the sol of PDMS–PZT composite was cast in between two silanized [9] glass plates prior to thermal curing as shown in the schematic of Fig. 1. The thickness of the composite film was kept constant at 1 mm using a spacer for all the samples. The volume fraction of the PZT was varied from 0 to 0.32. For comparing the significance of piezoelectric effect with passive mechanical

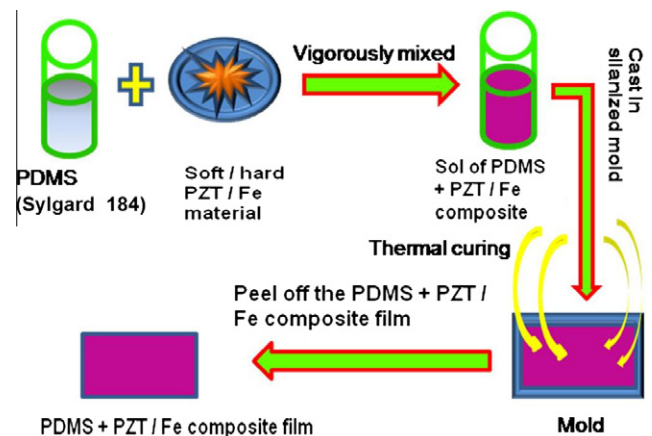


Fig. 1. Schematic of PZT (soft/hard/Fe filler) + PDMS composite synthesis process.

Table 1

Weight and corresponding volume percentage of various filler particles added to the PDMS matrix.

| Powder (Wt.%) | PZT [S] volume (%) | PZT [H] volume (%) | Fe volume (%) |
|---------------|--------------------|--------------------|---------------|
| 0 | 0 | – | – |
| 5 | 1 | – | – |
| 20 | 3 | – | – |
| 50 | 12 | – | – |
| 70 | 22 | 22 | 22 |
| 75 | 28 | 28 | 28 |
| 80 | 32 | 32 | 32 |

damping, two other materials (purchased from M/S Concord Electroceramic Ltd, New Delhi, India): (i) hard PZT (acceptor doping of iron manganese with grain size <1 μm) and lower coupling coefficient) and (ii) iron (metal) powder (Loba Chemie), of equal density (1.7 kg/m³) were dispersed in PDMS separately as shown in the schematic Fig. 1. Table 1 shows weight and the corresponding volume percentage of the filler particles used to prepare the composites.

2.2. Characterization of the PZT–PDMS composites

Viscoelastic properties and material loss factor of the composites (20 mm dia discs) were measured by the parallel plate method (Bohlin Rheometer, UK) in the frequency range of 0.1 to a maximum of 100 Hz, wherever possible, at initial strain and stress of 2% and 50 Pa respectively. For the vibration damping tests (Oberst beam configuration) [8], a steel beam of dimensions 50 \times 2.5 \times 0.1 cm was used as a cantilever base beam for bonding the PZT–PDMS composite sample. A sample of dimensions 5 \times 2.5 \times 0.13 cm was bonded at a distance of 40 mm from the fixed end of the cantilever beam using a very thin layer of insulating double-sided adhesive tape. To record the amplitude of tip vibration, a laser beam was focused near the free end of the beam and the vertical displacement of the sensing point was recorded using a laser sensor (Epsilon OPTO NCDT-1401). The free end of the cantilever beam was deflected by an initial displacement of 5 mm and left free to oscillate. The damping behavior of the beam with and without damping layer was analyzed. The overall loss factor for the unconstrained damping treatment is given by the following formulation.

$$\eta = (\eta_E)_2 e_2 h_2 (3 + 6h_2 + 4h_2^2) / [1 + e_2 h_2 (3 + 6h_2 + 4h_2^2)],$$

where,

$$(\eta_E)_2 = \text{loss-factor of the visco-elastic material} \quad (1)$$

e_2 = ratio of the storage modulus

h_2 = ratio of the thickness of the visco-elastic layer to the elastic layer

The overall loss-factor is measured by measuring the structural loss-factor from the frequency response of the systems and using the relationship that at resonance:

$$\eta = 2\zeta \quad (2)$$

where, ζ is the damping ratio.

By knowing, the over-all loss factor and all the other parameters of the above equation, we can obtain the loss-factor of the visco-elastic material.

For structural loss factor measurements, two opposite surfaces of the PZT–PDMS composite film were coated with aluminum using thermal evaporation. Then the samples were pasted on the FRP beam using double side adhesive copper tape and then the two electroded surfaces were connected to an external shunting circuit as shown in the Fig. 2. To record the output waveform a oscilloscope was used. Moreover, the free end of the cantilever

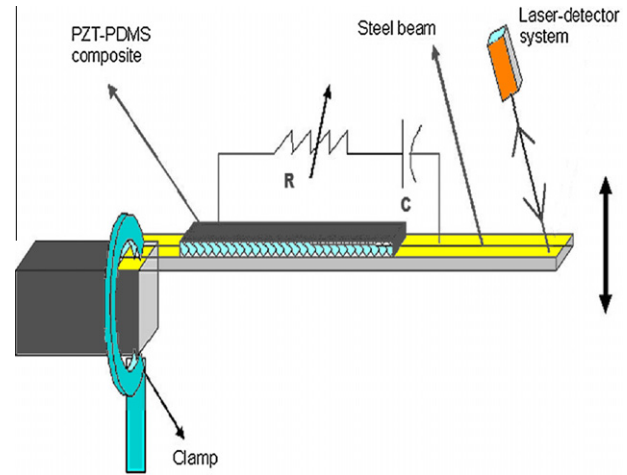


Fig. 2. Experimental setup used for the measurement of structural damping properties of PZT–PDMS composites.

was deflected through a predetermined distance of 5 mm and left free to oscillate.

Furthermore, for the active damping analysis maximum loss was calculated by attaching the electroded surface of the sample to an external shunting LCR circuit. The resistance of the LCR circuit was varied to obtain a maximum resonance between the LCR circuit frequency with internal charge generation frequency of the PZT–PDMS composite system. The adhesive tape of the material under test is another source of error. A sample was bonded from the fixed end of the cantilever beam using a very thin layer of insulating double-sided adhesive epoxy glue tape. Particularly, it was being kept to a minimum thickness as recommended in the ASTM E756 standard. To record the amplitude of the beam, a laser beam was incident at the free end of the beam and its output waveform was recorded using sensor. The complex modulus was computed at the temperature of 25 $^{\circ}\text{C}$. The experimental arrangement used for corona poling is shown in Fig. 3. In this technique, a high voltage DC field is applied between the Platinum electrode of the sharp tip and the PZT–PDMS composite sample. The Pt electrode acts as corona field intensifier, causing an ionization of surrounding gas molecules. ITO serves as one of the bottom electrodes. One surface of the sample to be poled is electroded and placed on a grounded metal plate. The charge from the tip is then sprayed onto the non-electroded surface. An optimal electric field of 1.6×10^5 V/cm is applied to the composite system at an elevated temperature of 90 $^{\circ}\text{C}$ to align the dispersed submicron filler particles. So that the effective field experienced by the filler particles is enough to align their magnetic domains. XRD spectra of soft/hard PZT/Fe filler dispersed in PDMS matrix before and after poling were taken on a PANalytical X'Pert PRO diffractometer to determine the orientation and shape of PZT particles, operating in the θ – 2θ Bragg configuration using Cu K α ($\lambda = 1.5405$ \AA) radiation. Data were collected at a scan rate of 0.02 s^{-1} and sampling interval of 0.0197 $^{\circ}$. The voltage was set at 45 kV with a 44 mA flux. FESEM images and atomic percentage composition of piezoelectric ceramic polymer composite were captured using a Carl Zeiss Supra 40 at 10 kV and Oxford EDAX for 50 s. The piezoelectric constants (d_{33}) and dielectric constant of soft/hard PZT–PDMS composites were computed by the Sensor 0643 Piezo-d Meter, (Sensor Technology Limited) and LCR meter (QuadTech 1693, Bolton, MA). It is very important to apply uniform stress to the sample due to the elastic behavior of PZT–PDMS composite. A house-fabricated half-sphere aluminum pillow was utilized during measurement to prevent the generation of stress gradient in the sample surfaces. The piezoelectric constant d_{33} was determined from the electric displacement calculated

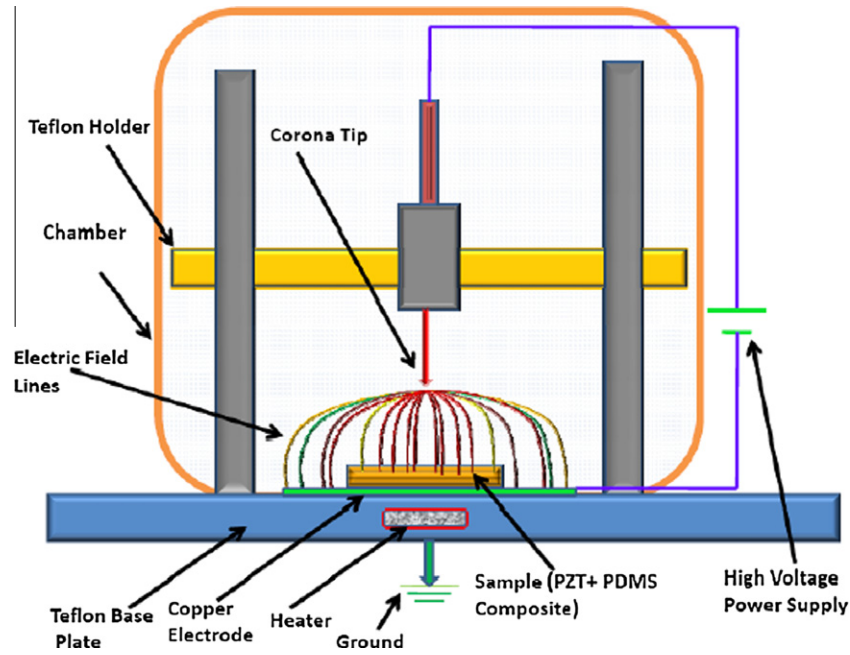


Fig. 3. Corona poling setup for soft/hard PZT filler dispersed in PDMS matrix for piezoelectric polymer composite.

through the polarization and the stress applied to the specimen. The piezoelectric constant was evaluated at the fixed resonance frequency of 200 Hz in this study.

3. Results and discussion

3.1. Material loss factor

The continuity of the two phases in a dispersion composite is denoted by $(\alpha-\beta)$ where $\alpha = 0, 1, 2$ and 3 indicates the connectivity of the dispersed particles with each other in 0 (isolated particles), one, two or three dimensions respectively, and as the second phase is generally continuous, $\beta = 3$. All the PZT–PDMS composites used for the present study are of type $0-3$, as the volume fractions of PZT in PDMS matrix are varied from 0 to 0.32 . Fig. 4 shows the storage shear modulus (G') in the natural logarithmic scale curve as a function of frequency for each of the PZT loading fraction. Since the elastic modulus of PZT (Epzt) is much higher in comparison to Epoly, it is observed that the elastic modulus (G') increases from 0.1 to 0.6 MPa with increase in PZT loading from 0 to 0.32 volume fraction. For 0.32 PZT volume fraction the G' curves show a broad

peak around 30 Hz. In case of lower volume fraction of PZT, G' is almost independent of the frequency. In contrast, as seen from Fig. 5, the shear viscous (loss) modulus (G'') curves in the natural logarithmic scale peak at 30 Hz for 0% PZT. In case of higher PZT fraction G'' increases by almost one order in magnitude along with a substantial increase in the width of the curve. Law et al. [8] studied the damping properties of $1-3$, $2-3$, $3-3$ (parallel model) as well as $0-1$, $0-2$ and $0-3$ (series model) composites, theoretically and experimentally. They have shown that the modulus ratio of the polymer (Epoly) to PZT particles (Epzt) plays an important role in the damping mechanism. They have also shown that piezo-damping in a series-composite is almost negligible for modulus ratio less than 0.1 , even for PZT fraction as high as 0.5 . Therefore, most of the series composites are useless in terms of piezo-damping. Here, we use a soft PZT–polymer combination such that its modulus ratio is very low ($E_{poly}/E_{pzt} \approx 0.001$). Similarly, in an independent work, rather than the piezoelectric effect, the higher density of PZT is found to be beneficial for increasing passive damping of the composite [23]. Therefore, the increase in loss factor of the PZT–PDMS composites studied here can be predominantly due to the viscous

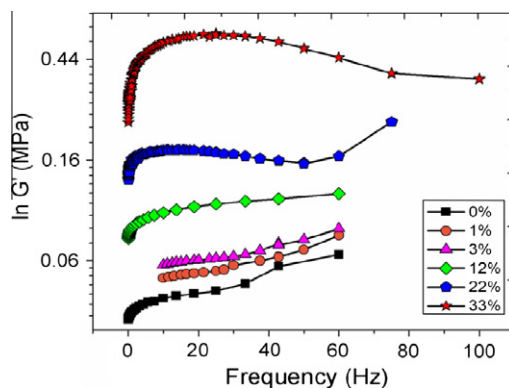


Fig. 4. Plot of storage modulus (G') vs. frequency of PZT–PDMS composites for PZT loading percentage of $0-32\%$.

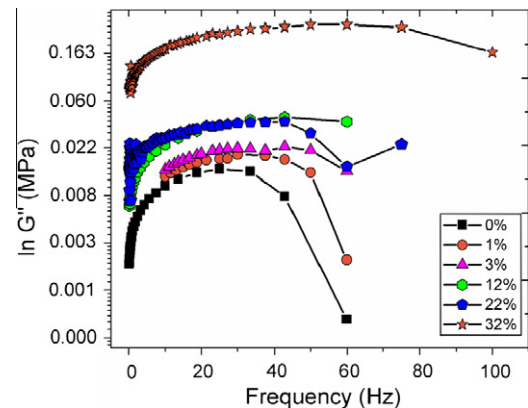


Fig. 5. Plot of loss modulus (G'') vs. frequency of PZT–PDMS composites for PZT loading percentage of $0-32\%$.

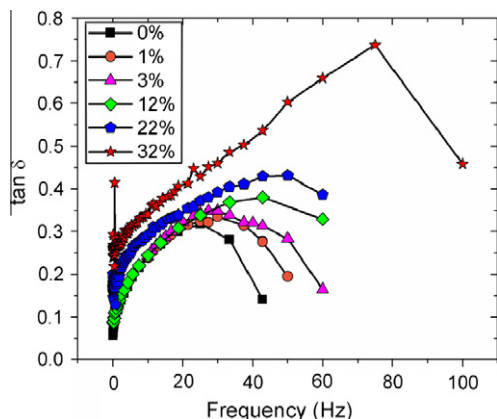


Fig. 6. Plot of material loss factor ($\tan \delta$) vs. frequency of PZT–PDMS composites for PZT loading percentage of 0–32%.

dissipation of energy in the form of passive damping, even though piezoelectric particles are dispersed in the matrix. The material loss factor ($\tan \delta$) vs. frequency curves as function of PZT volume fraction are shown in Fig. 6. As opposed to G' and G'' plots, $\tan \delta$ curves show maxima for every PZT fraction. However, most importantly, as PZT fraction in the composite increases, not only does the magnitude of $\tan \delta$ increase up to a maxima of 0.8 for 32% soft PZT volume, but the peak also broadens. This can be quantitatively expressed in terms of inverse quality factor, Q^{-1} , which is the measure of peak broadness and is equivalent to loss factor η [24]. As will be discussed later, η increases linearly from 0.003 to 0.0038 with increase in soft PZT volume fraction from 0 to 0.22 and then, abruptly increases to ~ 0.007 at 0.32 volume fraction. This behavior is clearly seen to be reflected in Fig. 6, where the peak corresponding to 0.32 volume fraction is very high as compared to other curves. These observations are consistent with studies on the loss factor peak of various viscoelastic materials by Pritz [25] where they report that the loss factor of a rubbery material may increase along with the peak broadening due to addition of filler particles. This property of the composite is of immense significance from the damping point of view. The broad peak of $\tan \delta$ indicates that the composite is capable of damping vibrations over a wider frequency range.

3.2. Material loss factor of hard PZT–PDMS and Fe–PDMS composites

Theoretically, the soft PZT particles have a large electro-mechanical coupling coefficient. A simple approach is proposed to investigate the contribution of electro-mechanical coupling coefficient of soft PZT towards the piezoelectric based damping of the PZT–PDMS composite system. Two solid filler particles, Fe and hard PZT particles, having same density (1.7 gm/cm^3) as soft PZT particles are dispersed by keeping its volume fraction between 0.22 and 0.32 in PDMS in place of soft PZT. In Fig. 7, the average storage (G') and loss (G'') modulus of hard PZT–PDMS composites are plotted on the primary Y-axis and $\tan \delta$ on the secondary Y-axis as a function of hard PZT particle volume percentage in the composite. It shows that G' increases from 0.15 to 0.35 MPa with increase in hard PZT volume percentage from 22 to 32%, similar to the case of soft PZT. However, maximum value of (G'') increases from 0.04 to 0.1 for increase in hard PZT volume fraction from 22% to 28%, but there is no significant increase or widening of the (G'') curve with further increase in hard PZT volume fraction. The varied behavior of (G') and (G'') as functions of hard PZT volume fraction also reflects in the material loss factor ($\tan \delta$). It is observed that the $\tan \delta$ curve shows a slightly higher maximum value

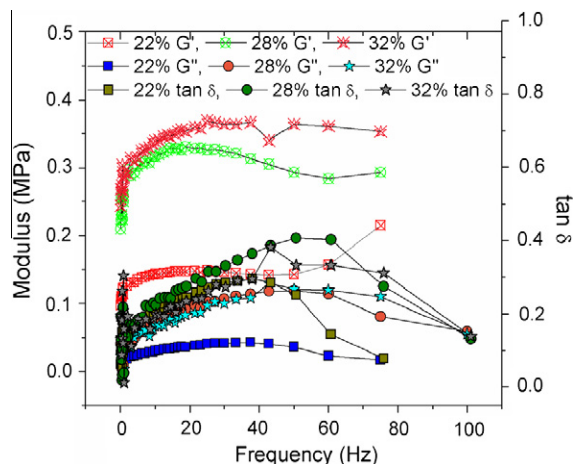


Fig. 7. Storage (G') and loss (G'') modulus and material loss factor ($\tan \delta$) of the hard PZT–PDMS composites as a function of frequency.

of 0.4 for 28% volume fraction as compared to 32%. This indicates that at higher volume fraction of hard PZT, the composite behaves more as an elastic material and its damping efficiency decreases. The rheological data of Fe–PDMS composite is shown in Fig. 8. It may be noted that of all the three filler particles used to prepare composites, the G' of Fe–PDMS composite is maximum as compared to the same volume fraction of soft and hard PZT–PDMS composites. G' of Fe–PDMS composite increases from 0.32 to 0.75 MPa as Fe volume fraction is increased from 0.22 to 0.32. However, the loss modulus G'' is observed to be maximum ($\sim 0.26 \text{ MPa}$) for 28% volume fraction of Fe particles and decreases to 0.10 MPa for 32% volume fraction indicating a decrease in the viscous energy dissipation capacity of the composite. The material loss factor ($\tan \delta$) increases continuously with the increase in the Fe volume percentage. However, for both hard PZT and Fe filler particulate composite, the maximum material loss factor at a particular volume fraction is nearly half that for the soft PZT composite. These rheological observations show that when the soft PZT particles are used as filler, the composite exhibits better damping properties. This is not just due to the density of filler particles, but may also result from a high electromechanical coefficient (k) of the soft PZT particles. A higher electromechanical coefficient indicates higher efficiency of the material to convert mechanical energy into electrical energy and vice versa. Thus, soft PZT particles convert

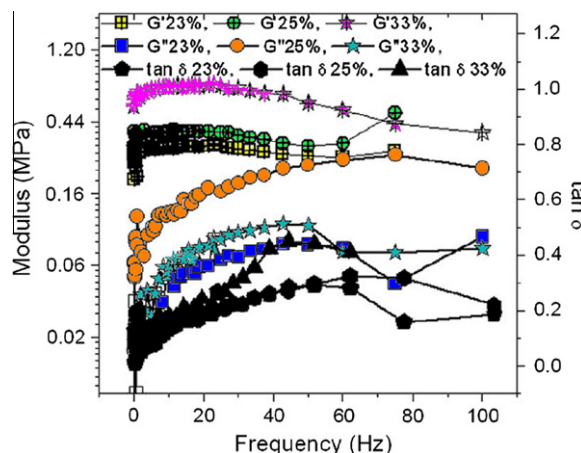


Fig. 8. Storage (G') and loss (G'') modulus and material loss factor ($\tan \delta$) of the Fe–PDMS composites as a function of frequency.

mechanical energy into electrical energy better than hard PZT and Fe particles, which increases the damping of the composite.

3.3. Poling of PZT–PDMS composite

A corona poling technique was employed to pole soft/hard PZT–PDMS composite at optimum electric field and at elevated temperature. The soft PZT–PDMS composite was found to be a promising composite material for damping, especially in terms of controllable flexibility by cross-linking. The damping efficiency of the composite could be increased by the poling of PZT particles in the composite [26]. The computation of the effective poling field required for PZT–polymer composite was performed by the Kura Kawa theory [27]. Here, the effective electric field E applied to the piezoelectric–polymer composite is computed by following relation:

$$\frac{E}{E_p} = \frac{2\varepsilon_1}{2\varepsilon_1 + \varepsilon_2 + \varphi(\varepsilon_1 - \varepsilon_2)} \quad (3)$$

where E is the effective electric field; E_p the applied electric field; ε_1 , the dielectric constants of PDMS; ε_2 the dielectric constants of PZT; φ the volume ratio of PZT filler in the PDMS matrix.

It indicates that the ceramic–polymer composite could be poled well under optimum conditions of electric field and temperature, which significantly influence the piezoelectric, dielectric and damping properties of the composite. However, PZT inherently possess dielectric and piezoelectric properties. Therefore, applying an electric field to the PZT ceramic, stored the charge in the form of complex permittivity. Hence, the real part normally is referred to as dielectric constant, while the loss tangent ($\tan \delta$) is equal to the ratio of imaginary/real part. For that reason, the application of poling electric field to the PZT ceramics, impact the dielectric and piezoelectric properties isotropically. Thus in general “free” and “clamped” dielectric constants computed at constant stress and strain are related through the electromechanical coupling factor (k). Fig. 9 shows the variations in the dielectric constants for composite system before and after poling. The general trend of increase in the dielectric constant of PZT–PDMS soft and hard composite with increase in the volume fraction of PZT is noted, though the effect is predominant in soft PZT composite. Also, these variations in the dielectric constants become more pronounced in soft as well as hard PZT–polymer composite after poling at the optimum electric field and temperature. It is perceived that there is approximately linear increase from 100 to 160 in the dielectric constant of soft-PZT–PDMS composite after the poling treatment,

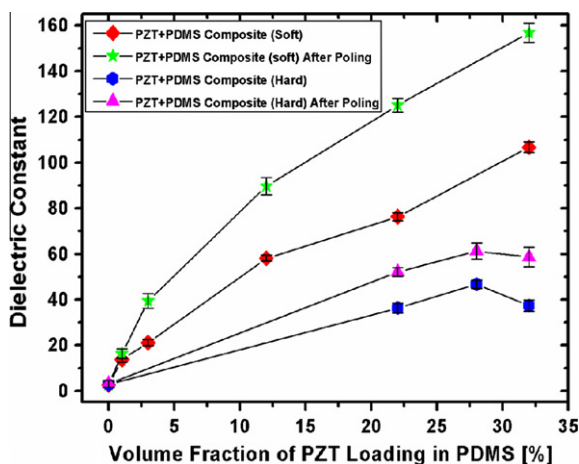


Fig. 9. Variation in the dielectric constant of soft/hard PZT–PDMS composite for different volume fractions of PZT in the PDMS matrix before and after poling.

while in case of hard PZT–PDMS composite, the reduction in dielectric constant is observed approximately at 28% or higher volume fraction of hard-PZT filler in PDMS matrix [28]. Furukawa et al. [18] have reported that the accumulation of ionic impurities at the interface of the PZT–PDMS composite and electrode polarization are responsible for the increase in dielectric constant at optimum poling condition of the PZT–polymer composite. It is observed that the rate of variation of the dielectric constant steadily increases with increase in the volume fraction of soft-PZT filler [28]. This might be because the poled PZT particles generate an internal field that favors the orientation of the PDMS molecules at optimum condition, resulting in an increase in the dielectric constant. This effect is more prominent and orderly in case of soft-PZT composite as compared to hard-PZT composite [29,30]. The shapes of soft and hard PZT filler particles observed by FESEM, as shown in Fig. 10A and B are, spheroidal or ellipsoidal. Fig. 10C and D shows the FESEM images of soft PZT filler volume fraction 0% and 22% respectively, dispersed in the PDMS matrix. Fig. 10C indicates the presence of a pure polymeric phase with chains of nanometric dimensions. With the addition of soft PZT filler particles, a distinct particulate phase with submicron particle size is observed. At 0.03 PZT volume fraction (FESEM images not shown), these particles are observed to be isolated in the matrix with very few particles seen at the surface. As the PZT volume fraction is increased from 0.03 to 0.22, a large number of particles become visible on the surface of the composite (Fig. 10D). This shows that as the PZT volume fraction is less than 0.5, soft/hard PZT filler particles do not connect with each other in any of the three dimensions throughout the matrix. Fig. 11 shows the increase in the piezoelectric coefficients (d_{33}) for 0–3 soft/hard PZT–PDMS composites as a function of the volume fraction of the filler in the PDMS matrix. In fact, the increase in d_{33} for soft-PZT PDMS composites is more significant as compared to that for hard-PZT–PDMS composites. In addition to this the charge retention competency of the soft/hard (PZT) fillers embedded in the PDMS matrix may not be only due to the conductivity of the PZT fillers but also due to charge retention capability of PDMS matrix. Because, there is a significant difference in charge storage behavior between PDMS/PZT filler composite materials and pure PDMS, it is reasonable to conclude that charges can penetrate (transport) with in the PDMS matrix and be trapped by the PZT fillers during the corona charging. The PDMS dielectric matrix may act as an energy barrier to prevent the injected charges in the PZT fillers from escaping to the outer environment. As a result, the PDMS/PZT fillers composite shows higher long-term surface charge stability than pure PDMS and have a marked improvement after poling. Furthermore, Fig. 12 shows the significant variation in d_{33} . It might be due to domain contribution for the composite system [31]. Moreover, the soft/hard PZT fillers have perovskite structure, in which without presence of external electric field (E^*), a uniform polarization develops along the domain walls at below Currie temperature (T_C) and could be switched by the influence of E^* . Especially, for the polycrystalline nature of PZT filler, because the domains within the grains could be permanently aligned or reoriented by mean of poling electric field. However, the PZT filler ceramics have a general chemical formula ABO_3 , represent the O (oxygen), A (cation with a larger ionic radius) and B (cation with a smaller ionic radius). Consequently, after the poling treatment of PZT/PDMS composite, the decrease in temperature of the composite system could be result the cubic paraelectric phase transfer into other phases like tetragonal, etc. due to the corner-linked oxygen octahedra, with the smaller cation filling the octahedral holes and the large cation filling the dodecahedral holes. In each phase, the dipole is generated by the displacement of the B-site ion along the same direction of the distortion and significantly influence the d_{33} piezoelectric co-efficient. This effect turns out to be more pronounced as a result of oxygen

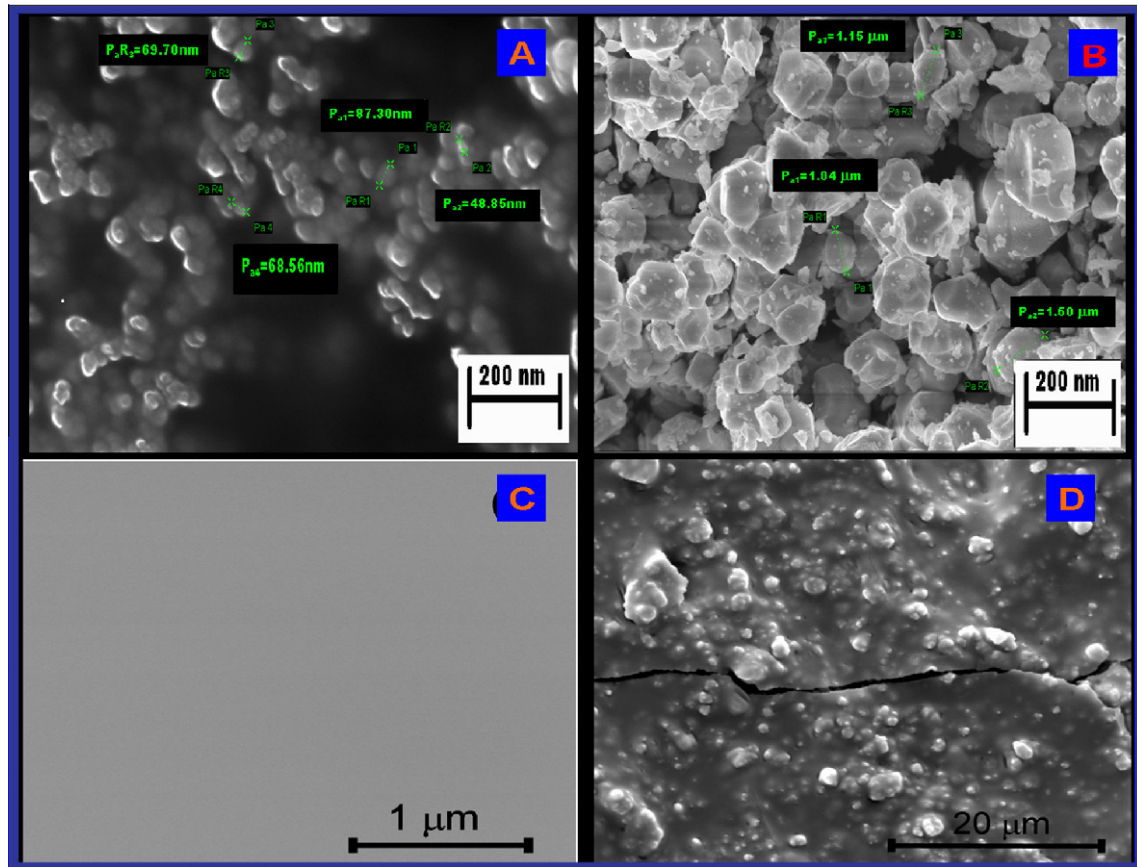


Fig. 10. FESEM images showing the particle shape and size of (A) soft-PZT, (B) hard-PZT particles and microstructure of PZT–PDMS composite with different PZT loading (C) 0 wt.%, and (D) 70 wt.% PZT. The crack in sample (D) is due to the sectioning of the sample for FESEM studies.

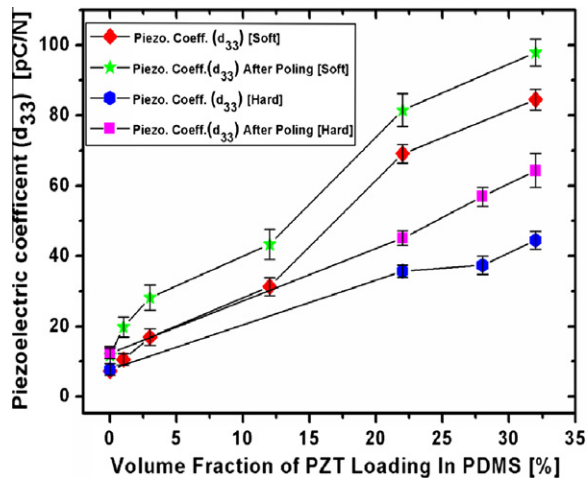


Fig. 11. Variation in piezoelectric coefficient (d_{33}) of PZT–PDMS composite with different volume fractions of soft and hard PZT particles before and after poling.

presence within host matrix, which influences the piezoelectric properties, due to domain wall motion. Hence, in case of PZT–polymer composite, the degree of domain contribution in the hard-PZT filler would be larger [32]. In the soft-PZTs, donors are added to reduce the concentration of oxygen vacancies, which are considered to be the origin of domain wall clamping. Therefore, domain walls move easily in the soft-PZT by the influence of E^* . On the other hand, acceptors are added to the hard-PZTs in order to increase the oxygen vacancy concentration results the clamping of domain

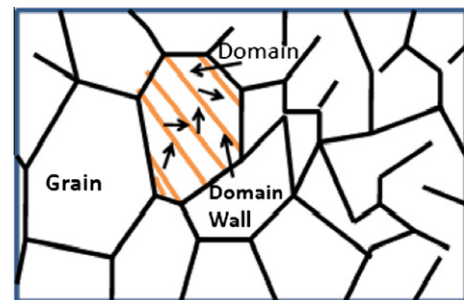


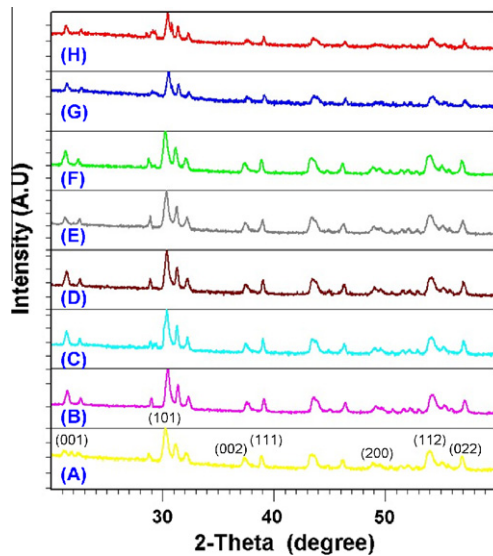
Fig. 12. Schematic diagram of defect dipoles and domain wall motion in the PZT–PDMS composite.

walls. It is to be noted that the effect of corona poling increases the oxygen composition of PDMS matrix, as shown in Table 2, due to the formation of hydroxyl group in PZT–PDMS composite [33]. In fact, the increase in oxygen composition in hard PZT filler composite is higher than that in soft PZT filler composite after the poling treatment. These results indicate that the oxygen concentration in hard PZT in a PDMS matrix is sufficient for clamping the domain walls. In addition to this presence of coexistence of local structures and stresses, the dielectric constant variation of PZT fillers attribute to the certain amount of pores, voids and strain/stress of the metastable state. Therefore in the present work the domain walls induced transformation occur in soft/hard PZT PDMS composite system matrix is more significantly due to the presence of oxygen within the host PDMS matrix. Thus, the soft PZT–PDMS

Table 2

Elemental atomic fraction composition of different constituents loading of soft/hard PZT in PDMS matrix before and after poling.

| Element | 12% soft PZT loading in PDMS matrix | 12% soft PZT loading after poling in PDMS matrix | 22% soft PZT loading in PDMS matrix | 22% soft PZT loading after poling in PDMS matrix | 22% hard PZT loading in PDMS Matrix | 22% hard PZT loading after poling in PDMS matrix |
|-----------|-------------------------------------|--|-------------------------------------|--|-------------------------------------|--|
| Carbon | 36.582 | 38.212 | 39.677 | 36.87 | 34.638 | 38.798 |
| Oxygen | 35.868 | 42.451 | 43.373 | 49.135 | 47.104 | 57.199 |
| Silicon | 27.072 | 37.744 | 10.169 | 14.291 | 10.648 | 22.917 |
| Titanium | 0.021 | 2.183 | 1.647 | 2.079 | 2.183 | 3.01 |
| Zirconium | 0.282 | 2.169 | 1.828 | 2.387 | 2.282 | 4.041 |
| Lead | 0.175 | 3.241 | 3.305 | 4.238 | 3.145 | 4.035 |

**Fig. 13.** XRD spectrum of soft PZT particles 12%, 22%, 28% and 32% volume fraction dispersed in PDMS matrix, (A), (C), (E) and (G) without poling and (B), (D), (F) and (H) with poling.

composites have sufficient domain wall motion, which results in the marked non-linearity of the composite system after poling and play a significant role in the damping. Table 2 shows the atomic percentage of diverse elements computed by EDAX mapping for composite system. Fig. 13 shows the XRD spectrum of various volume fractions of soft sub-micron PZT filler particles dispersed in PDMS matrix. As shown, the spectrum X-ray diffraction results indicate that the dispersed soft PZT particles in PDMS matrix have the lattice parameter $a = 5.84 \text{ \AA}$, $c = 14.41 \text{ \AA}$ and an increase in peak intensity due to the increase in volume fraction. Fig. 13A, C, E and G shows the relative percentage intensity variation 20.1, 23.1, 27.0 and 30.9 for (001), 17.5, 18.4, 24.6 and 28.6 for (002), 5.5, 5.9, 7.0 and 10.0 for (200) without poling for 12%, 22%, 28% and 32% volume fractions respectively of soft PZT particles dispersed in PDMS matrix. Similarly, Fig. 13B, D, F and H shows that the intensity variations after poling are 27.0, 27.3, 29.1 and 31.3 for (001), 19.5, 19.6, 25.6 and 29.0 for (002), 5.6, 6.1, 7.5 and 12.6 for (200) for 12%, 22%, 28% and 32% volume fraction respectively of soft PZT particles dispersed in PDMS matrix. These results indicate that dispersed soft PZT particles have tetragonal structures and (001) orientation. Generally, the orientation of particles are governed by energy minimization in terms of surface and strain energy of particles. Moreover, the increase in intensity after poling at optimum conditions reveals the enhancement in the number of alignments of dipole along (001) orientation within the composite [34]. The electric charge generated by these dispersed aligned particles can be dissipated by resistive shunting of the composite [7]. In addition, the strongest (101) PZT peak can still

be recognized for the spherical and ellipsoidal shapes of dispersed PZT particles that support the FESEM results. Hence, loss factor is measured by varying the shunting resistance from 0 to 1 k Ω for different volume fractions of soft PZT in PDMS matrix before and after poling treatment as shown in Fig. 14. When the PZT–PDMS composite bends during vibration, the PZT elements are strained and develop electric charges. This produces a resultant current through the resistors that dissipates energy in the form of heat and results in mechanical damping of the beam. Fig. 14 shows that loss factor shows a maximum for shunting resistance between 300–400 Ω and 700–900 Ω . It becomes more significant after the poling treatment. However, the variation in magnitude of the structural loss factor is lopsided. Still, it is interesting to note that higher loss factor η is achieved for soft PZT–PDMS after poling as compared to that achieved without poling due to the absence of effective dipole moment of PZT filler within the PDMS matrix. As PZT volume fractions vary from 3 vol.% soft PZT to 32 vol.% in the composite, there is an increase in η from 0.0011 to 0.0014 at 300 k Ω and 0.0012 to 0.0014 at 800 k Ω as indicated in Fig. 14a–d. Similarly, after poling treatment at the optimum condition, the increase in η is from 0.0015 to 0.0027 at 300 k Ω and from 0.0018 to 0.0025 at 800 k Ω as shown in Fig. 14e–h. Therefore, of all the composites studied, the PZT–PDMS composites fabricated using sub-micron PZT particles dispersed in PDMS matrix are found to be better suited as damping material. The difficulty with this type of composite, where the piezoelectric particles are smaller in diameter than the thickness of the polymer matrix, is that low permittivity polymer layers interleave the piezoelectric particles preventing saturation poling after the composite is formed. After some poling has been achieved, the interleaved compliant polymer attenuates the piezoelectric response of the composite. Therefore, poled composites are also made of Honeywell structures in which smaller PZT particles aggregate and form much larger conglomerates as shown in the FESEM images of Fig. 10. Since the piezoelectric particles redistribute from electrode to electrode, near-saturation poling can be achieved. The large rigid piezoelectric particles can transmit an applied stress leading to high d_{33} values as shown in Fig. 11. Moreover, the structural loss factor (η) of the soft PZT–PDMS composite is measured by the Oberst beam technique. The damping behavior of a mechanically excited steel beam, with and without damping layer is analyzed. The logarithmic decrement (δ) in the amplitude of the beam is calculated from the amplitude decrement between any chosen peak (d_i) and the subsequent n th peak (d_n) as per the relation ([35,36]):

$$\delta = [1/n] \ln [d_i/d_{i+n}] \quad (4)$$

This logarithmic decrement is directly related to the loss factor (η).

$$\eta \approx \delta/\pi \quad (5)$$

Fig. 15 shows the structural loss factor of soft PZT–PDMS composite as a function of soft PZT volume fraction η increases linearly from 0.003 to 0.0038 with increase in soft PZT volume fraction from 0 to 0.22. However, at 0.32 volume fraction, η increases abruptly to

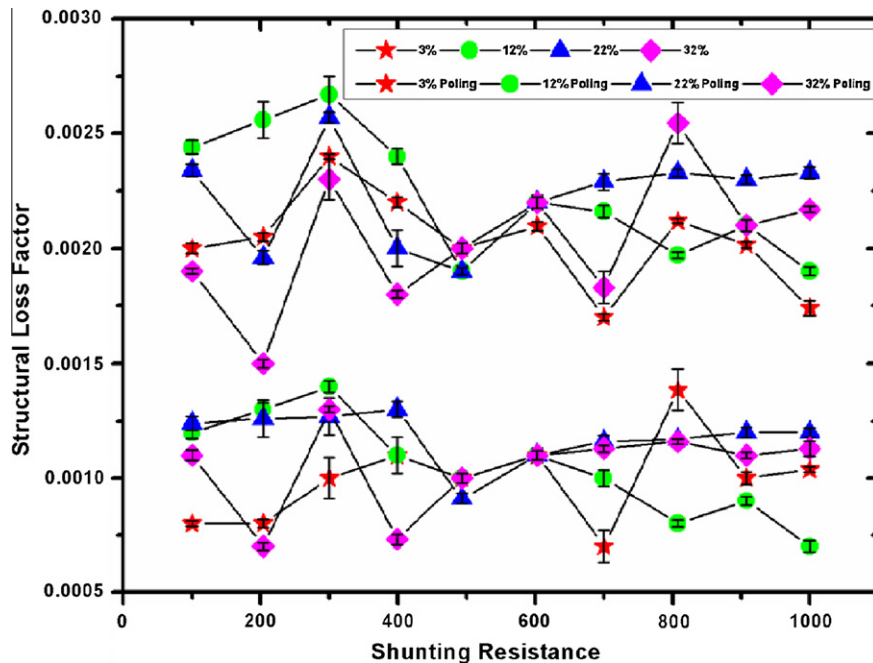


Fig. 14. Structural loss factor (η) of the PZT–PDMS composites for different PZT loading percentages as a function of shunting resistor connected between the electroded opposite surfaces of the composites before and after poling treatment.

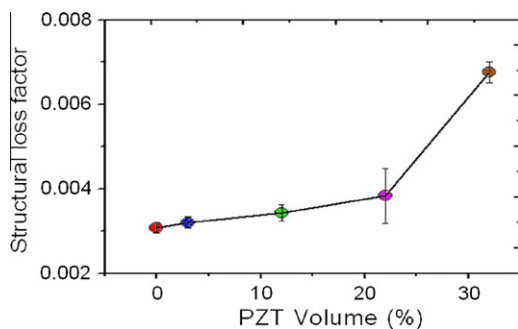


Fig. 15. Structural loss factor (η) of the PZT–PDMS composites as a function of loading percentage of PZT particles.

~ 0.007 . When filler particles are added to a polymer matrix, the friction produced between the filler particles and the PDMS matrix leads to energy dissipation, which is the main cause of the observed linear increase in the η . These results indicate that thin films of this composite would be more efficient in controlling the damping using a shunting resistor after poling as most of the PZT particles would then be having higher connectivity and presence on the surface of the film.

Additionally, for the consistency of measurement results for the material loss factor and structural loss factor is computed from the curve fitting for the real part of the modulus, by using the fractional model in Figs. 6 and 15. Thus, the measurements results of the damping coefficient are compared with the theoretical calculation using the local dispersion relation and compared with the theoretical values. Furthermore, the composite of piezoelectric polymer should have an optimal connectivity in such a way that the orientation of the piezoelectric phase within the polymer matrix is continuous from one electrode to the other to provide the continuity of electric flux required for saturation poling. The ceramic phase should also be oriented normal to the electroded surfaces for the transmission of mechanical stress and high piezoelectric response. This indicates that the properties of the composite are extremely position sensitive. Therefore, to make

an effective composite damper, designing of a composite entails not only the choice of component phases with the right properties, but also the coupling of materials in the optimal manner. The connectivity of each phase is of major importance since it controls the electric flux pattern and the mechanical stress distribution during damping. Also, the presence of polymer phase increases the elastic compliance, which enhances the applicability of the composite over complex surfaces of mechanical dimensions.

4. Summary

Mechanical vibration damping properties of soft PZT–Polydimethylsiloxane (PDMS) composites are studied with the help of rheometry and Oberst beam techniques. Use of PDMS as the polymer phase for improving the flexibility and passive damping of the vibrations is explored. Rheometric analyses have revealed that material loss factor as high as 0.7 is possible for 32 vol.% of soft PZT, while the structural loss factor measured by Oberst beam technique is ~ 0.007 . With increase in PZT fraction in the composite, not only have the maxima of the material loss factor curves increased, but the corresponding peaks have also broadened, indicating better damping over a larger range of frequencies. The dielectric constant and the piezoelectric coefficient (d_{33}) are observed to be higher for soft PZT based filler composite than for the hard, and both increase remarkably after poling. A resistively shunted composite shows nearly two fold increase in the structural loss factor of this composite because of the presence of soft PZT particles at the surface and this trend is more pronounced after poling. The mechanical vibration damping using soft PZT–PDMS composite would be higher than that using hard PZT and Fe; it could be tuned to the desired level and frequency by controlling the PZT volume fraction and the external shunting circuit.

Acknowledgments

Authors acknowledge the support of the Department of Science and Technology through the Thematic Unit of Excellence,

Nanoscience and Nanotechnology on Soft Nanofabrication formally known as DST Unit on Soft Nanofabrication at IIT Kanpur.

References

- [1] van den Ende DA, Bory BF, Groen WA, van der Zwaag S. Improving the d_{33} and g_{33} properties of 0–3 piezoelectric composites by dielectrophoresis. *J Appl Phys* 2010;107:024107.
- [2] Narayanan Manoj, Ma Beihai, Balu Balachandran U, Li Wei. Dielectric spectroscopy of $\text{Pb}_{0.92}\text{La}_{0.08}\text{Zr}_{0.52}\text{Ti}_{0.48}\text{O}_3$ films on hastelloy substrates with and without LaNiO_3 buffer layers. *J Appl Phys* 2010;107:024103.
- [3] Ahmad Zeeshan, Prasad Ashutosh, Prasad K. A comparative approach to predicting effective dielectric, piezoelectric and elastic properties of PZT/PVD composites. *Physica B* 2009;404:3637–44.
- [4] Hori M, Aoki T, Ohira Y, Yano S. New type of mechanical damping composites composed of piezoelectric ceramics, carbon black and epoxy resin. *Compos Part A: Appl Sci* 2001;32:287–90.
- [5] Uchino K, Sumita M, Sadanaga E. *Jpn Pat H3* 1991;188165:8–16.
- [6] Fries R, Moulson AJ. Fabrication and properties of an anisotropic PZT/polymer 0–3 composite. *J Mater Sci: Mater Electron* 1994;5:238–43.
- [7] Tanimoto T. A new vibration damping CFRP material with interlayers of dispersed piezoelectric ceramic particles. *Compos Sci Technol* 2007;67:213.
- [8] Law HH, Rossiter PL, Koss LL, Simon GP. *J Mater Sci* 1995;30:2648–55.
- [9] Tian Sheng, Cui Fangjin, Wang Xiaodong. New type of Piezo-damping epoxy-matrix composite with multi-walled carbon nanotubes and lead zirconate titanate. *Mater Lett* 2008;62:3859–61.
- [10] Reza SO, Fleming AJ. Piezoelectric transducers for vibration control and damping. UK: Springer; 2006.
- [11] Kang YK, Kim J and Choi SB. Passive and active damping characteristics of smart electro-rheological composite beams. *Smart Mater. Struct.* 2001;10:724–9.
- [12] Rujijanagul G, Boonyakul S, Tunkasiri T. Effect of the particle size of PZT on the microstructure and the piezoelectric properties of 0–3 PZT/polymer composites. *J Mater Sci Lett* 2001;20:1943.
- [13] Satish B, Sridevi K, Vijaya MS. Study of piezoelectric and dielectric Properties of ferroelectric PZT–polymer composites prepared by hot-press technique. *J Phys D: Appl Phys* 2002;35:2048–50.
- [14] Takeuchi H, Nakaya C. Polymer composites for medical ultrasonic probes. *Ferroelectrics* 1986;68:53–61.
- [15] Newham RE, Skinner DP, Cross LE. *Mater Res Bull* 1978;13:525.
- [16] Shrout TR, Schulze WA, Biggers JV. *Mater Res Bull* 1979;14:1553.
- [17] Safari A, Halliyal A, Bowen LJ, Newham RE. Flexible composite transducers. *J Am Ceram Soc* 1982;65:207.
- [18] Furukawa T, Ishida K, Fukada E. Piezoelectric properties in the composite systems of polymers and PZT ceramics. *J Appl Phys* 1979;50(7):4904–11.
- [19] Wilder EA, Guo S, Lin-Gibson S, Fasolka MJ, Stafford CM. *Macromolecules* 2006;39:4138.
- [20] Gonuguntla M, Sharma A, Subramaniam SA. *Macromolecules* 2006;39:3365–8.
- [21] Bourim El Mostafa, Tanaka Hidehiko, Gabbay Maurice, Fantozzi Gilbert, Cheng Bo Lin. Domain wall motion effect on the anelastic behavior in lead zirconate titanate piezoelectric ceramics. *J Appl Phys* 2002;91:6662.
- [22] Tsurumi Takaaki, Sasaki Tsutomu, Kakemoto Hirofumi, Harigai Takakiyo, Wada Satoshi. Domain contribution to direct and converse piezoelectric effects of PZT ceramics. *Jpn J Appl Phys* 2004;43(11A):7618.
- [23] Grewe MG, Gururaja TR, Newnham RE, In: Ultrasonic symposium: institute of electrical and electronic engineers; 1989;713–6.
- [24] Zhang J, Perez RJ, Lavernia EJ. Documentation of damping capacity of metallic, ceramic and metal–matrix composite materials. *J Mater Sci* 1993;28:2395–404.
- [25] Pritz T. Loss factor peak of viscoelastic materials: magnitude to width relations. *J Sound Vib* 2001;246(2):265–80.
- [26] Ren Q, Xu D, Chow YT, Lu ZH, Ma CB, Zhang GH, et al. Preparation and characterization of a poled nanocrystal and polymer composite $\text{PbTiO}_3/\text{PEK-C}$ film for electro-optic applications. *Appl Phys A* 2003;76:183–6.
- [27] Liu WC, Li AD, Tan J, Wu D, Ye H, Ming NB. Preparation and characterization of poled nanocrystal and polymer composite PZT/PC films. *Appl Phys A* 2005;81:543–7.
- [28] Takahiro Yamakawa, Masako Kataoka, Norikazu Sashida. Influence of poling conditions on the piezoelectric properties of PZT ceramics. *J Mater Sci Mater Electron* 2000;11:425–8.
- [29] Venkatragavaraj E, Satish B, Vinod PR, Vijaya MS. Piezoelectric properties of ferroelectric PZT–polymer composites. *J Phys D: Appl Phys* 2001;34:487–92.
- [30] Higashihata Y, Yagi T, Sako. Piezoelectric properties and applications in the composite system of vinylidene fluoride and trifluoroethylene copolymer and PZT ceramics. *J Ferroelectrics* 1986;68:63.
- [31] Masuda Y. Variation of dielectric constant affected by domain structure and electric-field-induced strain in ferroelectric ceramics. *Jpn J Appl Phys* 1994;33:5549.
- [32] Narita Fumio, Shindo Yasuhide, Mikami Masaru. Analytical and experimental study of nonlinear bending response and domain wall motion in piezoelectric laminated actuators under ac electric fields. *Acta Mater* 2005;53:4523.
- [33] Hillborg H, Gedde UW. Hydrophobicity recovery of polydimethylsiloxane after exposure to corona discharges. *Polymer* 1998;39(10):1991.
- [34] Shi Wei, Guo Shiyi, Fang Changshui, Xu Dong. Poling and properties of nano-composite thin film PT/PEK-C. *J Mater Sci* 1999;34:5995.
- [35] Thomson WT. Vibration theory and applications. Prentice-Hall; 1965. p. 45.1.
- [36] Kulkarni MM, Bandyopadhyaya R, Bhattacharya B, Sharma A. Microstructural and mechanical properties of silica–PEPEG polymer composite xerogels. *Acta Mater* 2006;54:5231–40.